IOWA STATE UNIVERSITY
Digital Repository

1-1-1974

A multipurpose computer code for the UTR-10 reactor

Min-jen Min-jen
Iowa State University

www.manaraa.com

A multipurpose computer code

for the UTR-10 reactor

by

Min-jen Chen

A Thesis Submitted to the

Graduate Faculty in Partial Fulfillment of

The Requirements of the Degree of

MASTER OF SCIENCE

Department: Chemical Engineering and
             Nuclear Engineering

Major: Nuclear Engineering

Iowa State University
of Science and Technology
Ames, Iowa

1974

TABLE OF CONTENTS

I. INTRODUCTION

Various computer codes have been developed for the determination of nuclear reactor parameters. Some of them have been widely used and present a high level of confidence. These include LEOPARD [1], FOG [2], and PERT [3]. For example, LEOPARD and FOG have been utilized in the determination of reactor parameters in the preliminary safety analysis report of a nuclear power plant [4].

The objective of the author's work was to investigate the nuclear parameters of the UTR-10 reactor by these codes. The investigation included the calculation of neutron flux, criticality search, reactivity coefficients, prompt neutron lifetime and effective delayed neutron fraction.

When a large number of problems are to be solved, an economically feasible way should be considered. The primary concern in this study is to present the developed code and show its ability and cost to solve problems.

A multigroup, one-dimensional code called SCORP (single-step calculation of reactor parameters) was developed to investigate the reactor parameters.

II. LITERATURE SURVEY

As a result of modern computers, an enormous number of computer
codes have been developed. Neutron fluxes, adjoint fluxes, various
criticality searches, reactivity changes, reactor parameters, neutron
lifetimes and effective delayed neutron fractions are found analytically
either by using two-dimensional digital programs or by reducing the
two-dimensional problems to pseudo-one-dimensional digital computer
problems which can be solved by one-dimensional digital computer
programs. The latter method is, in practice, the only one that is
economically feasible when a large number of problems are to be
solved. To illustrate: a two-dimensional problem having the same
mesh spacing as a one-dimensional problem would take some 100-1000
times as long to complete [5].

A. The LEOPARD Code

The LEOPARD code [1] determines fast and thermal spectra, using
only basic geometry, composition and temperature data, based on a
MUFT-SOFOCATE [6, 7] model as modified by Arnold [8] and again by
Strawbridge [9].

LEOPARD output includes nuclear parameters for three fast groups,
a combined one fast group, and a thermal group. As originally written,
LEOPARD included a punched output option for CANDLE [10] or AIM-5 [11].

As reported by Munson [12], the LEOPARD code has been extensively
modified. The modifications allow the code to be run on an IBM-360,
add a slab option to the cell geometry possibilities, and delete punched

output options that readied the LEOPARD data for use in CANDLE or AIM-5.
As a result of these modifications, the code description by Barry [1]
does not fully describe the code available at Iowa State University.
This description of LEOPARD does not include the fuel depletion option
because this option was not explored as a part of this work.

As reported by Strawbridge [9], LEOPARD represents an improvement
over the previous method as evidenced by a reduction in the standard
deviation about the mean for several groups of experiments of particular
interest in the design of pressurized water reactors. The LEOPARD
code was found to be in good agreement with a more rigorous calcula-
tion which requires approximately 50 times more computer time.

B. The FOG Code

The FOG code [2] is a collection of control programs utilizing
a basic set of subroutines for use in performing various reactor
calculations based upon the solution of the one-dimensional neutron
diffusion equation.

The FOG code can handle from one to four energy groups, up to
239 space points, and up to 40 regions. Neutrons are permitted to
scatter only from a given energy group to the next lower group. The
principal options available in the various programs are:

(a) Choice of three geometries.

(b) Calculation of the fluxes and the multiplication factor.

(c) "One iteration" problems.

(d)   Choice of one of nine possible sets of boundary conditions
for homogeneous calculations or of eight possible sets for
nonhomogeneous calculations.

(e)   Criticality searches on the transverse buckling, homogeneous
poison, critical radius, location of a poison boundary, and
location of the fuel boundary.

(f)   Calculation of the adjoint flux.

(g)   A buckling iteration calculation for a fully-reflected, right
circular cylinder.

A detailed derivation of the numerical method used in FOG was
presented by Munson [12]. Munson also presented flux distributions
of the UTR-10 reactor from earlier models and from the calculations
with the FOG code.

By one-dimensional computer code [1] , Nowark and Chow [13] gave
the results of their calculation for the UTR-10. Their analyses
were based on two-group diffusion theory for the three regions of the
reactor, i.e., the coupling region, the fuel tank and the thermal
column. Campos [14] presented his measurement of the flux distribu-
tions in the thermal column of the UTR-10. Their results have been
used as a check on the results of the present work.

C.   The PERT Code

The PERT code is a perturbation theory code basically designed
to perform several calculations based on punched-card output from the
AIM-5, AIM-6, or FOG codes. The punched-card output contains the

fluxes, adjoint fluxes, various cross sections and diffusion coefficients. The purpose of PERT is:

(a)   To compute the relative change in reactivity due to a perturbation in macroscopic cross sections and/or in the diffusion coefficient.

(b)   To compute the prompt neutron lifetime and effective delayed neutron fraction.

(c)   To weigh cross sections either with fluxes and adjoint fluxes or with fluxes only.

The program allows 40 regions, 238 mesh points, 18 energy groups, and 5 fissionable species present.

Since the reactivity coefficients and prompt neutron lifetime are of extreme interest in reactor kinetic behavior, many papers on these investigations of the UTR-10 reactor have been reported and these results have been used as a check of the output of PERT.

Based on two group perturbation theory, void coefficient, temperature coefficient, and prompt neutron lifetime have been reported by American Standard [15]. The magnitude of β/ℓ has been reported by Nodean [16], Chan [17], Merritt [18], and Nabavian [19].

III. THEORY

A. One-Dimensional Diffusion Theory and Mathematical Method

The steady state diffusion equation can be written as

$$D\nabla^2\phi - \Sigma_a\phi + S = 0 \tag{1}$$

In reactor calculations, it is usually necessary to consider only three coordinate systems: namely, rectangular, cylindrical, and spherical coordinates. In these coordinate systems, assume the fluxes are symmetric, ∇^2 is given by

$$\text{rectangular:} \quad \nabla^2 = \frac{\partial^2}{\partial x^2} + \frac{\partial^2}{\partial y^2} + \frac{\partial^2}{\partial z^2}$$

$$\text{cylindrical:} \quad \nabla^2 = \frac{\partial^2}{\partial r^2} + \frac{1}{r}\frac{\partial}{\partial r} + \frac{\partial^2}{\partial z^2} \tag{2}$$

$$\text{spherical:} \quad \nabla^2 = \frac{\partial^2}{\partial r^2} + \frac{2}{r}\frac{\partial}{\partial r}$$

Consider a rectangular reactor with extrapolated dimensions a, b and c, for the purpose of reducing the three-dimensional problem to one-dimensional problem, we introduce the transverse buckling B^2 in the following way:

$$B^2 = B_y^2 + B_z^2 \tag{3}$$

where $B_y^2 = -\frac{1}{\phi}\frac{\partial^2\phi}{\partial y^2}$ and $B_z^2 = -\frac{1}{\phi}\frac{\partial^2\phi}{\partial z^2}$, for a critical bare reactor,

$B_y^2 = (\frac{\pi}{b})^2$ and $B_z^2 = (\frac{\pi}{c})^2$. Then Eq. (1) can be written as

$$D\frac{\partial^2\phi}{\partial x^2} - DB^2\phi - \Sigma_a\phi + S = 0 \tag{4}$$

The transverse buckling of the various geometries considered in this system are summarized in Table 1, with this definition, Eq. (4) can be generalized as

$$D(\frac{\partial^2 \phi}{\partial r^2} + \frac{P}{r} \frac{\partial \phi}{\partial r}) - DB^2\phi - \Sigma_a\phi + S = 0 \tag{5}$$

where   P = 0 for rectangular geometry

        = 1 for cylindrical geometry

        = 2 for spherical geometry.

Table 1. Transverse bucklings of critical base reactors (all dimensions are extrapolated)

Geometry	Dimension	Direction	Transverse buckling
Rectangular parallelepiped	a ✕ b ✕ c	x	$(\frac{\pi}{b})^2 + (\frac{\pi}{c})^2$
		y	$(\frac{\pi}{a})^2 + (\frac{\pi}{c})^2$
		z	$(\frac{\pi}{a})^2 + (\frac{\pi}{b})^2$
Cylinder	Radius R	r	$(\frac{\pi}{H})^2$
	Height H	z	$(\frac{2.4048}{R})^2$
Sphere	Radius R	r	0

Now, with the definition of transverse buckling, the generalized k-group one-dimensional diffusion equation is written

$$- D(r)_i [\frac{\partial^2}{\partial r^2} + \frac{P}{r} \frac{\partial}{\partial r}] \phi(r)_i + B^2(r)_i D(r)_i \phi(r)_i$$

$$+ \Sigma_a(r)_i \phi(r)_i + t_i \Sigma_p(r)_k \phi(r)_i + \Sigma_R(r)_i \phi(r)_i$$

$$= \chi_i \frac{G(r)}{\lambda} + \Sigma_R(r)_{i-1} \phi(r)_{i-1} \qquad \text{for } 1 \leq i \leq k \qquad (6)$$

The symbols are defined as

ϕ_i = neutron flux in i-th group

D_i = diffusion coefficient for the i-th group

B_i^2 = transverse buckling for the i-th group

$(\Sigma_a)_i$ = absorption cross section for the i-th group

$(\Sigma_p)_k$ = poison cross section in the thermal group

t_i = ratio of poison cross section in group i to thermal

poison cross section

$(\Sigma_R)_{i-1}$ = removal cross section in group i - 1 to group i

χ_i = the integral of the fission spectrum over the lethargy

range represented by group i

r = radius measured from the origin

P = 0 for plane geometry

= 1 for cylindrical geometry

= 2 for spherical geometry

$$G(r) = \sum_{i=1}^{k} (\nu\Sigma_f(r))_i \phi(r)_i$$

$$\lambda = \int_0^R G(r) dV_P$$

with $dV_P = dr$, when $P = 0$;

$dV_P = 2\pi r dr$, when $P = 1$;

$dV_P = 4\pi r^2 dr$, when $P = 2$.

Equation (6) can be solved numerically by a sequence of difference equations [20] based on given boundary conditions.

Let $\Sigma_T(r)_i = D(r)_i B^2(r)_i + \Sigma_a(r)_i + t_i(\Sigma_P)_k + \Sigma_R(r)_i;$ (7)

$$f(r)_i = \chi_i \frac{G(r)}{\lambda} + \Sigma_R(r)_{i-1}\phi(r)_{i-1}$$ (8)

Equation (6) can be written

$$\frac{1}{r^P}[\frac{\partial}{\partial r}(r^P D_i \frac{\partial\phi_i}{\partial r})] = (\Sigma_T)_i\phi_i - f_i$$ (9)

We consider the interval $0 \leq r \leq R$ and divide the interval into N subintervals and denote the interpolation points as r_k, $0 \leq k \leq N$. The spacing is denoted by $\Delta r_k = r_{k-1} - r_k$, and are not necessarily equal. However, we assume that an interpolation point falls at each interface between regions. We now integrate Eq. (9) from $r_{k-\frac{1}{2}}$ to $r_{k+\frac{1}{2}}$ to obtain

$$r^P D_i \frac{\partial\phi_i}{\partial r}\Big|_{r_{k+\frac{1}{2}}} - r^P D_i \frac{\partial\phi_i}{\partial r}\Big|_{r_{k-\frac{1}{2}}}$$

$$= \int_{r_k}^{r_{k+\frac{1}{2}}} r^P[(\Sigma_T)_i\phi_i - f_i]dr + \int_{r_{k-\frac{1}{2}}}^{r_k} r^P[(\Sigma_T)_i\phi_i - f_i]dr$$ (10)

Since the materials may be discontinuous, the integrand is factored into portions whose integrands are continuous.

We expand the integrals on the right and obtain

$$\int_{r_k}^{r_{k+\frac{1}{2}}} r^P[\Sigma_T)_i\phi_i - f_i]dr = [\Sigma_T(r_k^+)_i\phi(r_k)_i - f(r_k^+)_i]r_k^P \frac{\Delta r_k}{2}$$ (11)

$$\int_{r_{k-\frac{1}{2}}}^{r_k} r^P [(\Sigma_T)_i \phi_i - f_i] dr = [\Sigma_T(r_k^-)_i \phi(r_k)_i - f(r_k^-)_i] r_k^P \frac{\Delta r_k}{2} \tag{12}$$

with accuracy $0(\Delta r)^2$. The + sign denotes the value of the factors obtained as $r \rightarrow r_k$ from the right while the - sign denotes the value from the left. For r_k not on an interface, the integral becomes

$$\int_{r_{k-\frac{1}{2}}}^{r_{k+\frac{1}{2}}} r^P [(\Sigma_T)_i \phi_i - f_i] dr$$

$$= [\Sigma_T(r_k)_i \phi(r_k)_i - f(r_k)_i] r_k^P \left(\frac{r_{k+1} - r_{k-1}}{2}\right) \tag{13}$$

The derivative terms can be approximated as

$$\left.\frac{\partial \phi_1}{\partial r}\right|_{r_{k+\frac{1}{2}}} = \frac{\phi_{i,k+1} - \phi_{i,k}}{r_{k+1} - r_k} \tag{14}$$

$$\left.\frac{\partial \phi_i}{\partial r}\right|_{r_{k-\frac{1}{2}}} = \frac{\phi_{i,k} - \phi_{i,k-1}}{r_k - r_{k-1}} \tag{15}$$

of accuracy $0(\Delta r)^2$. Using the difference approximations Eq. (11), Eq. (12), Eq. (14), and Eq. (15) in Eq. (10), we obtain a 3-point difference equation

$$a_{i,k} \phi_{i,k+1} - b_{i,k} \phi_{i,k} + c_{i,k} \phi_{i,k-1} = - \omega_{i,k} \tag{16}$$

where the coefficients are given by

$$a_{i,k} = \frac{r_{k+\frac{1}{2}} D_{i,k+\frac{1}{2}}}{\Delta r_k}$$

$$c_{i,k} = \frac{r_{k-\frac{1}{2}} D_{i,k-\frac{1}{2}}}{\Delta r_{k-1}}$$

$$\omega_{i,k} = \frac{r_k^P}{2} [\Delta r_k f_i(r_k^+) + \Delta r_{k-1} f_i(r_k^-)]$$

$$b_{i,k} = \frac{r_{k+\frac{1}{2}} D_{i,k+\frac{1}{2}}}{\Delta r_k} + \frac{r_{k-\frac{1}{2}} D_{i,k-\frac{1}{2}}}{\Delta r_{k-1}}$$

$$+ \frac{r_k}{2} [\Sigma_T(r_k^+)_i \Delta r_k + \Sigma_T(r_k^-)_i \Delta r_{k-1}]$$

Equation (16) can also be derived by central difference scheme as shown by Flatt [21].

B. Multigroup Adjoint Flux and Perturbation Analysis

The K-group diffusion equation with downward transfer coefficients can be written as [22]

$$D_i \nabla^2 \phi_i - (\Sigma_a)_i \phi_i - \sum_{n=i+1}^{K} \Sigma_{i \to n} \phi_i + \chi_i \sum_{n=1}^{K} (\nu \Sigma_f)_n \phi_n$$
$$+ \sum_{n=1}^{i-1} \Sigma_{n \to j} \phi_n = 0 \qquad (17)$$

As is known, Eq. (17) may be expressed as a matrix form $(M)(\phi) = 0$, where (ϕ) is the column vector consisting of the components ϕ_i. The corresponding adjoint equation for the adjoint flux, $(M^+)(\phi^+) = 0$, is directly obtainable by interchange of rows and columns to form (M^+)

Thus with two groups,

$$D_1 \nabla^2 \phi_1 - \Sigma_{a1} \phi_1 - \Sigma_{1 \to 2} \phi_1 + \chi_1 (\nu \Sigma_f)_1 \phi_1 + \chi_1 (\nu \Sigma_{f2}) \phi_2 = 0 \qquad (18)$$

$$D_2 \nabla^2 \phi_2 - \Sigma_{a2} \phi_2 + \Sigma_{1 \to 2} \phi_1 + \chi_2 (\nu \Sigma_f)_1 \phi_1 + \chi_2 (\nu \Sigma_{f2}) \phi_2 = 0 \qquad (19)$$

may be written in matrix form as

$$\begin{pmatrix} (D_1\nabla^2 - \Sigma_{a1} - \Sigma_{1\to2} + \chi_1\nu\Sigma_{f1}) & (\chi_1\nu\Sigma_{f1}) \\ (\chi_2\nu\Sigma_{f2} + \Sigma_{1\to2}) & (D_2\nabla^2 - \Sigma_{a2} + \chi_2\nu\Sigma_{f2}) \end{pmatrix} \begin{pmatrix} \phi_1 \\ \phi_2 \end{pmatrix} = 0$$

(20)

The matrix adjoint, (M^+), is then

$$(M^+) \equiv \begin{pmatrix} (D_1\nabla^2 - \Sigma_{a1} - \Sigma_{1\to2} + \chi_1\nu\Sigma_{f1}) & (\chi_2\nu\Sigma_{f1} + \Sigma_{1\to2}) \\ (\chi_1\nu\Sigma_{f2}) & (D_2\nabla^2 - \Sigma_{a2} + \chi_2\nu\Sigma_{f2}) \end{pmatrix}$$

(21)

and the adjoint equations are

$$D_1\nabla^2\phi_1^+ - \Sigma_{a1}\phi_1^+ - \Sigma_{1\to2}\phi_1^+ + \chi_1\nu\Sigma_{f1}\phi_1^+ + \chi_2\nu\Sigma_{f1}\phi_2^+ + \Sigma_{1\to2}\phi_2^+ = 0 \quad (22)$$

$$D_2\nabla^2\phi_2^+ - \Sigma_{a2}\phi_2^+ + \chi_2\nu\Sigma_{f2}\phi_2^+ + \chi_1\nu\Sigma_{f2}\phi_1^+ = 0 \quad (23)$$

Extension to more energy groups is evident.

In general, then, for a critical system

$$(M)(\phi) = 0 \quad (24)$$

and

$$(M^+)(\phi^+) = 0 \quad (25)$$

The matrix (M) may, however, be expressed as the sum of production and loss matrices:

$$(M) \equiv (P) + (L) \quad (26)$$

In two groups, for example,

$$(P) = \begin{pmatrix} (X_1 \nu\Sigma_{f1}) & (X_1 \nu\Sigma_{f2}) \\ (X_2 \nu\Sigma_{f2}) & (X_2 \nu\Sigma_{f2}) \end{pmatrix} \tag{27}$$

$$(L) = \begin{pmatrix} (D_1\nabla^2 - \Sigma_{a1} - \Sigma_{1\to2}) & 0 \\ (\Sigma_{1\to2}) & (D_2\nabla^2 - \Sigma_{a2}) \end{pmatrix} \tag{28}$$

For a critical system, then,

$$(P + L)(\phi) = 0 \tag{29}$$

In general, for a critical or noncritical system,

$$(\frac{P}{k} + L)(\phi) = 0 \tag{30}$$

k is the multiplication factor and (ϕ) are the solutions with matrices (P) and (L). Also as $k^+ = k$, the general adjoint equation is

$$(\frac{P^+}{k} + L^+)(\phi^+) = 0 \tag{31}$$

By use of the flux and adjoint equation, and the adjoint properties

$$\iint (\phi^+)(P)(\phi)dVdE = \iint (\phi)(P^+)(\phi^+)dVdE \tag{32}$$

and

$$\iint (\phi^+)(L)(\phi)dVdE = \iint (\phi)(L^+)(\phi^+)dVdE \tag{33}$$

it may be shown that

$$k = \frac{\iint (\phi^+)(P)(\phi)dVdE}{\iint (\phi^+)(L)(\phi)dVdE} \tag{34}$$

By this equation, the reactivity change may be estimated for systems having matrix operators (P') and (L') differing slightly from (P) and (L) by replacement of the primed matrices for the unprimed in the integrals, the flux and adjoints being known solutions of the unprimed matrix diffusion equations.

The perturbation expression for fractional change in reactivity is then obtainable by differentiation (square brackets here represent the integrations) where $(\delta\phi^+)$ and $(\delta\phi)$ are neglected:

$$\frac{\delta k}{k} = \frac{[(\phi^+)(\delta P)(\phi)]}{[(\phi^+)(P)(\phi)]} - \frac{[(\phi^+)(\delta L)(\phi)]}{[(\phi^+)(L)(\phi)]} \tag{35}$$

Equation (34) further reduces to

$$\frac{\delta k}{k} = \frac{[(\phi^+)(\delta P - \delta L)(\phi)]}{[(\phi^+)(P)(\phi)]} \tag{36}$$

if k is unity for the unperturbed system. The denominator is the volume-energy integral of importance-weighted fission neutrons in the entire system before the perturbation.

The forms of the integrals for multigroup perturbation analysis may be illustrated by the explicit expressions for two groups. The denominator is then

$$[(\phi^+)(P)(\phi)] = \int \phi_1^+ \chi_1 \nu_1 \Sigma_{f1} \phi_1 dV + \int \phi_1^+ \chi_1 \nu_2 \Sigma_{f2} \phi_2 dV$$

$$+ \int \phi_2^+ \chi_2 \nu_1 \Sigma_{f1} \phi_1 dV + \int \phi_2^+ \chi_2 \nu_2 \Sigma_{f2} \phi_2 dV \tag{37}$$

The numerator terms are

$$[(\phi^+)(\delta P)(\phi)] = \int \phi_1^+ \chi_1 \delta(\nu_1 \Sigma_{f1})\phi_1 dV + \int \phi_1^+ \chi_1 \delta(\nu_2 \Sigma_{f2})\phi_2 dV$$

$$+ \int \phi_2^+ \chi_2 \delta(\nu_1 \Sigma_{f1})\phi_1 dV + \int \phi_2^+ \chi_2 \delta(\nu_2 \Sigma_{f2})\phi_2 dV \qquad (38)$$

and

$$-[(\phi^+)(\delta L)(\phi)] = - \int \phi_1^+ \delta(\Sigma_{a1})\phi_1 dV - \int \phi_2^+ \delta(\Sigma_{a2})\phi_2 dV$$

$$- \int \phi_1^+ \delta(\Sigma_{1 \to 2})\phi_1 dV + \int \phi_2^+ \delta(\Sigma_{1 \to 2})\phi_1 dV$$

$$- \int \delta D_1 \nabla \phi_1^+ \cdot \nabla \phi_1 dV - \int \delta D_2 \nabla \phi_2^+ \cdot \nabla \phi_2 dV \qquad (39)$$

Equation (38) represents the group fission effects. The first two terms of Eq. (39) represent the group absorption effects. The third and fourth terms taken together represent the effect of the net difference in importance of neutrons transferred, i.e.,

$$\int (\phi_2^+ - \phi_1^+) \delta(\Sigma_{1 \to 2})\phi_1 dV$$

This indicates the physical meaning of the adjoint function. Thus, $\delta(\Sigma_{1 \to 2})\phi_1$ corresponds to a neutron sink or negative source in group 1 and simultaneously a neutron source in group 2. The importance of this exchange in its effect upon reactivity, and hence upon the overall neutron inventory, is determined by the relative values of the adjoints. The last two terms of Eq. (39) give the importance of leakage effects in the perturbed region.

Equation (36), Eq. (37), Eq. (38), and Eq. (39) can be expressed in a generalized form as

$$\frac{\delta K}{K} = F - A - T - D \tag{40}$$

where

$$F = \int_V dV \int_E dE\phi(r, E) \left[\iint_{E'} dE' \chi(E')\phi^+(r, E') \right] \delta(\nu\Sigma_f)/I$$

$$A = \int_V dV \int_E dE\phi(r, E)\phi^+(r, E)\delta(\Sigma_a)/I$$

$$T = \int_V dV \int_E dE\phi(r, E) \int_{E'} dE' [\phi^+(r, E) - \phi^+(r, E')]\delta(\Sigma_{E\rightarrow E'})/I$$

$$D = - \int_V dV \int_E dE\delta(D(r, E))\nabla\phi(r, E) \cdot \nabla\phi^+(r, E)/I$$

$$I = \int_V dV \int_E dE\phi(r, E) \left[\iint_{E'} dE' \chi(E')\phi^+(r, E') \right] \nu\Sigma_f(r, E)$$

C. Prompt Neutron Lifetime and Effective Delayed Neutron Fraction

Calculation of prompt neutron lifetime can proceed by use of fluxes and adjoint fluxes of the unperturbed system. In this method [23]

$$\ell_P \int_E \int_V \phi^+L\phi dVdE = \int_E \int_V \frac{\phi^+\phi}{v} dVdE \tag{41}$$

where ℓ_P represents the prompt neutron lifetime and v represents the neutron velocity. The neutron lifetime multiplied by the loss rate of importance equals the total importance of all the neutrons, i.e., $\iint \phi^+NdEdV$, where $N = \frac{\phi}{v}$.

For a critical system the loss rate of importance equals the production rate of importance, the latter being an easier quantity to calculate. Thus

$$\ell_p = \frac{\displaystyle\int_E \int_V \frac{\phi^+\phi}{v}\, dVdE}{\displaystyle\int_E \int_V \phi^+ P\phi\, dVdE} \tag{42}$$

Equation (42) can be expressed in multigroup notation as

$$\ell_p = \frac{\displaystyle\int_V \sum_{i=1}^{K} \left(\frac{\phi_i^+\phi_i}{v_i}\right) dV}{\displaystyle\int_V \sum_{j=1}^{K} \chi_j \sum_{i=1}^{K} [(\nu\Sigma_f)_i\, \phi_i^+\phi_i]\, dV} \tag{43}$$

The group velocity v_i may be estimated by

$$\frac{1}{v_i} = \frac{\displaystyle\int_{\text{group } i} \frac{\phi(E)\, dE}{v(E)}}{\displaystyle\int_{\text{group } i} \phi(E)\, dE} \tag{44}$$

where $\phi(E)$ is assumed to follow a 1/E distribution within the epithermal groups.

The delayed neutrons play an important role in reactor kinetic behavior. The fissioning of U-238 emits much more delayed neutrons per fission that U-235, hence the calculation of effective delayed neutron fraction is necessary.

The quantity β_{eff}, the effective delayed neutron fraction, may also be calculated by use of the group flux and adjoint solutions of the diffusion equation [23],]24]. β_{eff} is given by $\beta_{eff} = D/(P + D)$,

where D is a quantity proportional to the worth of all the delayed

neutrons and P is a quantity proportional to the worth of all prompt

neutrons.

In the multigroup notation and for the case of, for example, the

fissionable species U-235 and U-238, D and P have the explicit forms:

$$D = \beta^{25} \int_V [\sum_j (\nu\Sigma_f)_j^{25} \phi_j][\sum_j \chi_j^{25D} \phi_j^+] dV$$

$$+ \beta^{28} \int_V [\sum_j (\nu\Sigma_f)_j^{28} \phi_j][\sum_j \chi_j^{28D} \phi_j^+] dV$$

$$P = [1 - \beta^{25}] \int_V [\sum_j (\nu\Sigma_f)_j^{25} \phi_j][\sum_j \chi_j \phi_j^+] dV$$

$$+ [1 - \beta^{28}] \int_V [\sum_j (\nu\Sigma_f)_j^{28} \phi_j][\sum_j \chi_j \phi_j^+] dV$$

The fission fraction of the delayed and prompt neutrons are normalized

separately by

$$\sum_j \chi_j^{25D} = 1; \quad \sum_j \chi_j^{28D} = 1; \quad \sum_j \chi_j = 1$$

The β^{25} and β^{28} of the individual fissionable species may be

evaluated from experimental values of n/F, the number of delayed

neutron per fission, and of $\bar{\nu}$, the mean value of the number of total

neutrons emitted per fission. For example, some listed experimental

values for the case of fast neutron fission are [25], [26]:

$$(\frac{n}{F})^{25} = 0.0165; \quad \bar{\nu}^{25} = 2.56; \quad \beta^{25} = 0.00645$$

$$(\frac{n}{F})^{28} = 0.0412; \quad \bar{\nu}^{28} = 2.62; \quad \beta^{28} = 0.0157$$

The delayed neutron fraction for U-238 is seen to be much larger than that of U-235.

IV. DEVELOPMENT OF THE SCORP CODE

The SCORP code, embodies the basic features of the FOG and PERT codes, and it provides a convenient tool for the UTR-10 reactor calculations.

The structure of SCORP is similar to that of FOG, however, there are some significant differences. This code excluded the options of spherical and cylindrical geometries, buckling iteration, poison boundary search, and fuel loading search which are not necessary for the UTR-10 reactor calculations. The main additions to SCORP are the calculations of reactivity change, beta-effective, and prompt neutron lifetime. The purpose of these modifications and additions was to allow simple-step calculation of many UTR-10 reactor parameters of interest, with minimum required input data and at less cost.

The program allows 40 regions, 238 mesh points, 4 energy groups, one group of down scatter and no up scatter. The perturbation is required to be within one region.

A. Procedures for Solutions

1. Flux calculation

With the input data of cross sections, reactor size, etc., the calculation proceeds from the reactor outer boundary to the inner boundary, starting with the highest energy group. After the sweep through all groups is completed, a new fission source is calculated from the resultant fluxes. The source is then normalized to a total of one fission neutron in the reactor. This normalization is given as

$$\int_0^R \sum_i (\nu\Sigma_f)_i \phi_i \, dr = 1.0$$

For the first two inner iterations, the new normalized source distribution is used to calculate the fluxes in the following iteration. In the third and subsequent iterations, the starting source at a point for the following iteration is obtained by linear extrapolation from the previous iteration. The equation is

$$S_{n,j} = S'_{n,j}(1 + \theta) - \theta \cdot S_{n,j-1} \qquad (0 < \theta < 1)$$

where $\quad S_{n,j-1}$ = the normalized source at point n after j - 1st iteration

$S'_{n,j}$ = the source guess for iteration j

$S_{n,j}$ = the normalized source at point n after j-th iteration.

In this program θ is set to 0.8.

Inner iterations are continued until the convergence criterion is met, or until the inner iteration limit is exceeded.

When the inner iteration loop calculation has converged, the code exits to a buckling search or adjoint flux calculation as specified by the user.

2. Buckling search

The buckling search proceeds through successive trials of transverse buckling to reach a specified eigenvalue, which need not be equal to 1.0. When the convergence criterion is met, the code exits to the adjoint flux calculation.

3. <u>Adjoint flux calculation</u>

Options are available such that the user may specify real solutions only, real and adjoint solutions, or adjoint solution only. No search options may be used on an adjoint solution.

When an adjoint solution is specified, the scattering matrix is transposed, X and $\nu\Sigma_f$ are interchanged, and the group structure is inverted, so that the lowest energy group becomes group 1. Then starts the same procedure as flux calculation.

4. <u>Perturbation calculation</u>

Based on the theory presented in Section II, the program proceeds to compute $\Delta K/K$, β_{eff} and ℓ. Options are available such that the user may specify the calculation of $\Delta K/K$, or β_{eff} and ℓ or both.

The perturbation is required to be within one region, however, variation in the boundaries of the perturbed region is permitted.

The trapezoidal rule for integration is employed here. The same denominator is employed in all cases.

The prompt neutron spectrum X is assumed to be material independent.

The detailed description of input data for SCORP is presented in Appendix A. In Appendix B, the description of output is presented. The sample data of the SCORP code is presented in Appendix C.

V. RESULTS AND DISCUSSION

A. The UTR-10 Reactor Parameter Calculation

Nuclear parameters, necessary inputs to FOG and PERT, were calculated by LEOPARD code. LEOPARD output includes nuclear parameters for three fast groups, a combined one fast group, and a thermal group. The prototype reactor model used in this study is shown in Fig. 1 and represents a one-dimensional idealization of the UTR-10 reactor.
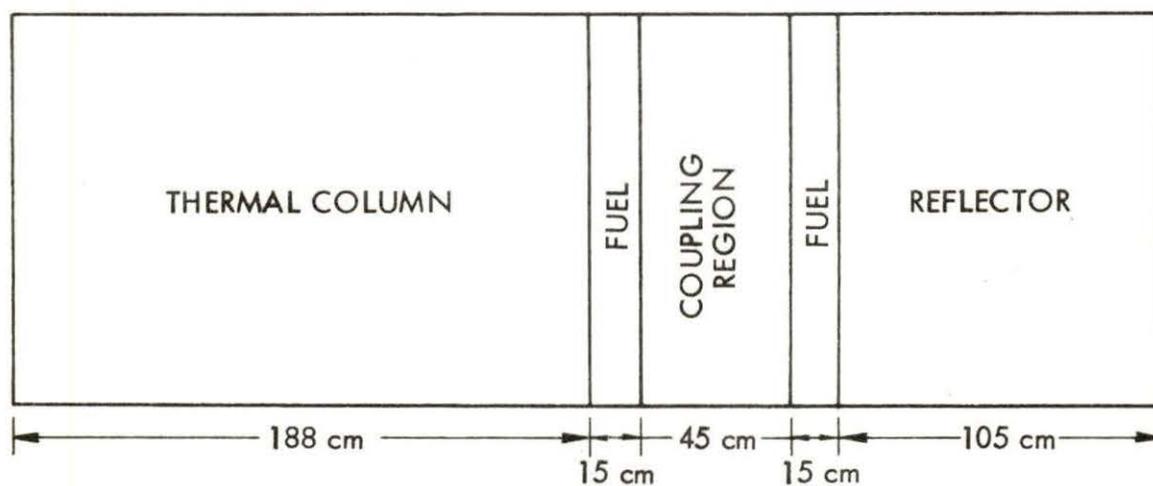
Fig. 1. Dimensions of UTR-10 reactor model

The fuel slab has 12 fuel elements. The fuel element containing 12 fuel plates is made of 93.25% enriched UAl_4. The fuel plate is 0.2032 cm thick. The water gap between fuel plates is 1.016 cm thick.

The calculated results of the UTR-10 reactor parameters are given in Table 2 to 10. The cut-off energy for the three fast groups are 8.21×10^5 eV, 5.53×10^3 eV, and 0.625 eV respectively [4].

Tables 2 to 7 present the reactor parameters at various temperatures and void fraction. Table 8 gives the reactor parameter of fuel

plate region. In this calculation we consider the fuel plate is a
unit cell and no moderator included. Tables 9 and 10 present the
reactor parameters of water and graphite respectively.

Table 2. Reactor parameters of core region coolant temperature =
89 °F. No void formation

	D	Σ_a	$\Sigma_{s,i\to i-1}$	$\nu\Sigma_f$
1st group	2.02553	0.00126	0.09337	0.00031
2nd group	1.10455	0.00024	0.12230	0.00039
3rd group	0.60465	0.00500	0.12055	0.00595
A combined fast group	1.12926	0.00207	0.03737	0.00208
Thermal group	0.19372	0.05998		0.09030

Table 3. Reactor parameters of core region coolant temperature =
109 °F. No void formation

	D	Σ_a	$\Sigma_{s,i\to i-1}$	$\nu\Sigma_f$
1st group	2.03175	0.00126	0.09302	0.00031
2nd group	1.10821	0.00025	0.12181	0.00039
3rd group	0.68726	0.00503	0.12004	0.00596
A combined fast group	1.30054	0.00208	0.03720	0.00209
Thermal group	0.19667	0.05900		0.08892

Table 4. Reactor parameters of core region coolant temperature =
89 °F. 1% of void

	D	Σ_a	$\Sigma_{s,i \to i-1}$	$\nu\Sigma_f$
1st group	2.04163	0.00126	0.09248	0.00031
2nd group	1.11398	0.00025	0.12105	0.00039
3rd group	0.69133	0.00502	0.11928	0.00595
A combined fast group	1.30726	0.00208	0.03696	0.00208
Thermal group	0.19577	0.05981		0.09029

Table 5. Reactor parameters of core region coolant temperature =
89 °F. 5% of void

	D	Σ_a	$\Sigma_{s,i \to i-1}$	$\nu\Sigma_f$
1st group	2.10951	0.00121	0.08892	0.00031
2nd group	1.15366	0.00025	0.11609	0.00039
3rd group	0.71939	0.00499	0.11427	0.00595
A combined fast group	1.35348	0.00205	0.03535	0.00208
Thermal group	0.20445	0.05915		0.09024

Table 6. Reactor parameters of core region coolant temperature = 89 °F. 10% of void

	D	Σ_a	$\Sigma_{s,i \to i-1}$	$\nu\Sigma_f$
1st group	2.20147	0.00116	0.08447	0.00031
2nd group	1.20747	0.00025	0.10988	0.00039
3rd group	0.75784	0.00494	0.10801	0.00594
A combined fast group	1.41626	0.00201	0.03334	0.00207
Thermal group	0.21641	0.05831		0.09016

Table 7. Reactor parameters of core region coolant temperature = 85 °F. 15% of void

	D	Σ_a	$\Sigma_{s,i \to i-1}$	$\nu\Sigma_f$
1st group	2.30306	0.00110	0.08002	0.00031
2nd group	1.26672	0.00025	0.10369	0.00039
3rd group	0.80063	0.00490	0.10177	0.00594
A combined fast group	1.48561	0.00198	0.03135	0.00207
Thermal group	0.22985	0.05475		0.09004

Table 8. Reactor parameters of fuel plate. Fuel plate temperature = 89 °F

	D	Σ_a	$\Sigma_{s,i \to i-1}$	$\nu\Sigma_f$
1st group	2.64489	0.00171	0.01780	0.00259
2nd group	2.04438	0.00304	0.00037	0.00524
3rd group	3.14424	0.00838	0.00095	0.01377
A combined fast group	2.17595	0.00293	0.229×10^{-4}	0.00515
Thermal group	1.35996	0.18302		0.37109

Table 9. Reactor parameters of water. Water temperature = 89 °F

	D	Σ_a	$\Sigma_{s,i \to i-1}$	$\nu\Sigma_f$
1st group	2.26557	0.00142	0.10452	0.0
2nd group	1.09904	0.00001	0.14997	0.0
3rd group	0.59131	0.00094	0.15107	0.0
A combined fast group	1.34507	0.00081	0.04867	0.0
Thermal group	0.15502	0.01880		0.0

Table 10. Reactor parameters of graphite

	D	Σ_a	$\Sigma_{s,i \to i-1}$	$\nu\Sigma_f$
1st group	2.28926	0.613×10^{-8}	0.02440	0.0
2nd group	1.05132	0.165×10^{-9}	0.01117	0.0
3rd group	0.93488	0.955×10^{-8}	0.00656	0.0
A combined fast group	1.12622	0.608×10^{-8}	0.00366	0.0
Thermal group	0.99571	0.00032		0.0

B. Thermal Neutron Flux Distribution in the UTR-10 Reactor

To demonstrate the ability of the FOG code to solve reactor
criticality problems, several calculations of the UTR-10 flux distribu-
tion are presented. The problems were run by using the data from
LEOPARD.

Figures 2 and 3 are FOG calculated thermal flux distribution in
both core tanks. Figures 4 and 5 are FOG calculated thermal fluxes
with one fuel plate withdrawn from the fuel element. In a heterogeneous
reactor such as UTR-10, thermal flux depression should occur in the
fuel plate. Figures of thermal flux distribution (Figs. 2 to 5) show
this depression in the output from the FOG code.

Figure 6 shows the thermal flux in the thermal column calculated
by FOG, the theoretical calculation by Nowark and Chow [13], and the
experimental result by Campos [14]. It shows that the results are
in slight disagreement. The higher attenuation of FOG output is
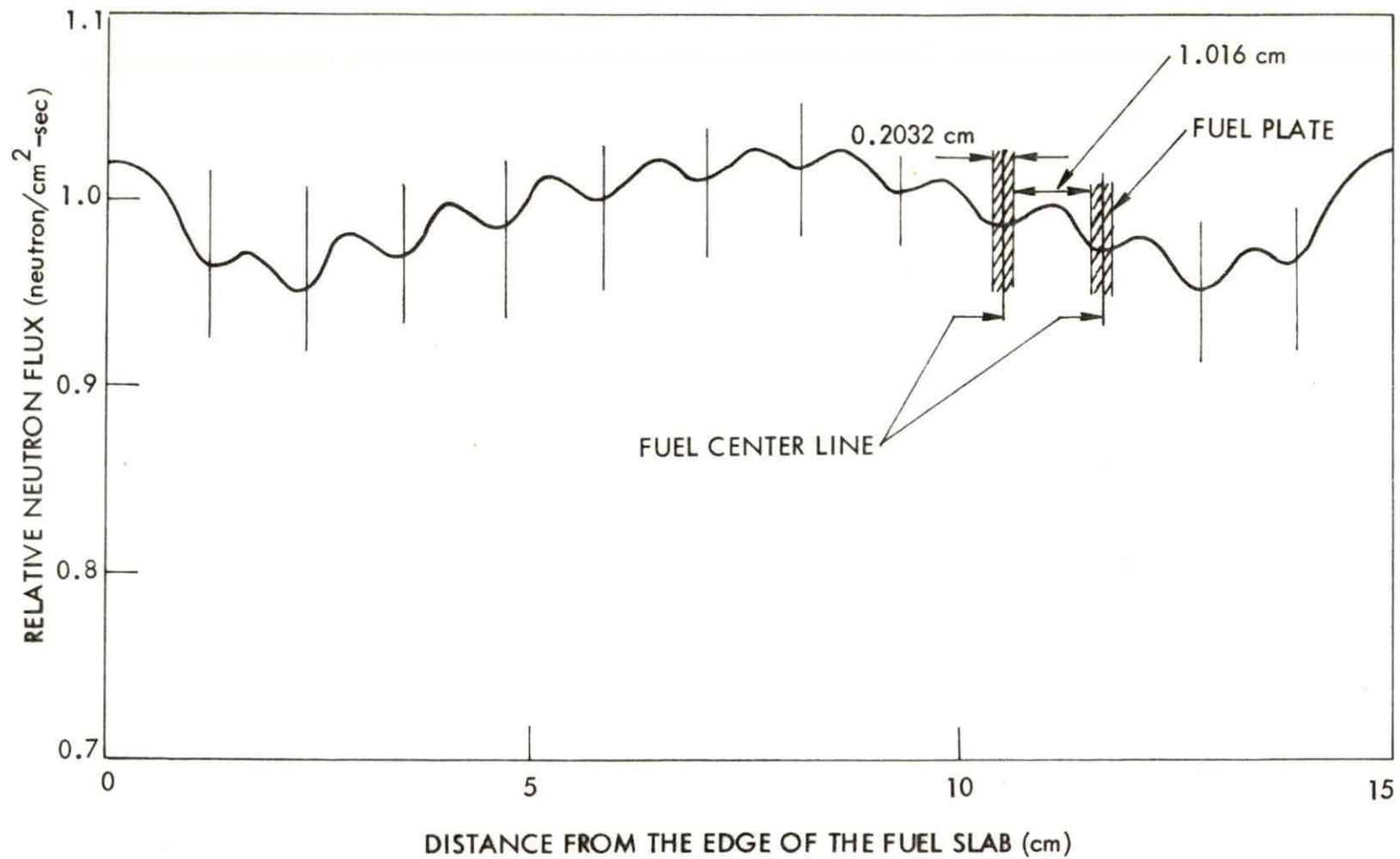
Fig. 2. Thermal neutron flux distribution in the fuel element of the North Core.
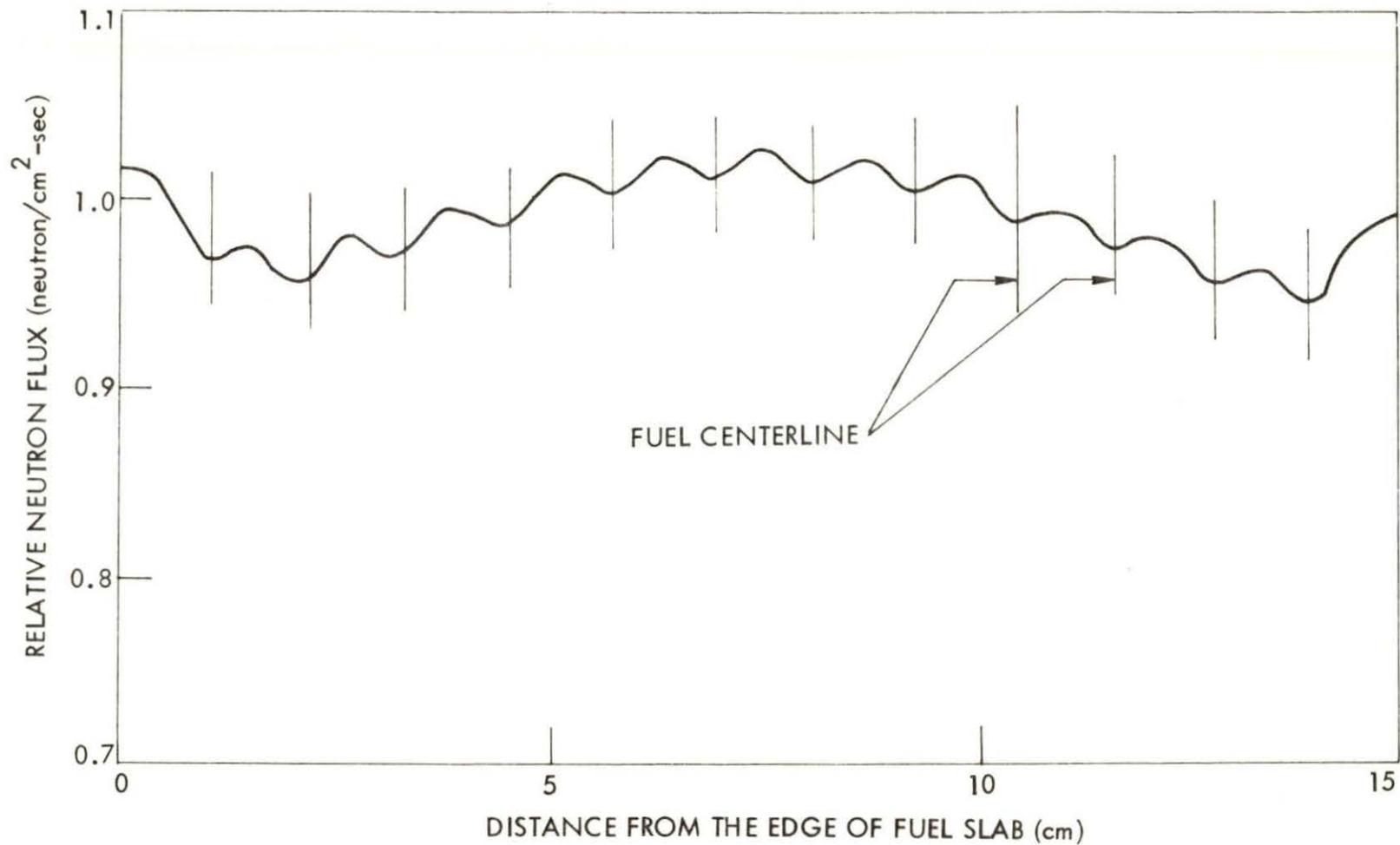
Fig. 3. Thermal neutron flux distribution in the fuel element of the South Core
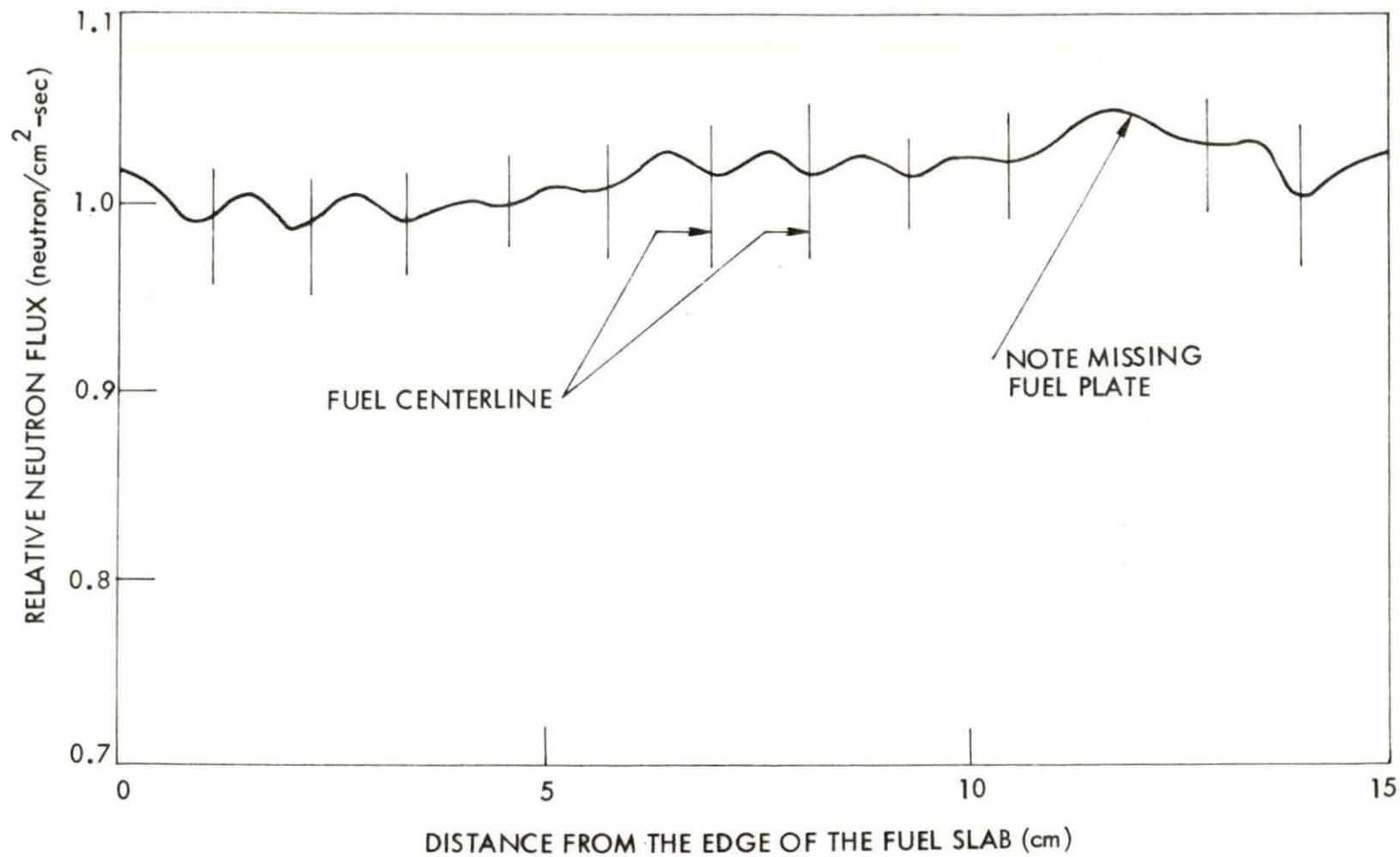
Fig. 4. Thermal neutron flux distribution in the fuel element of the North Core with one fuel plate withdrawn
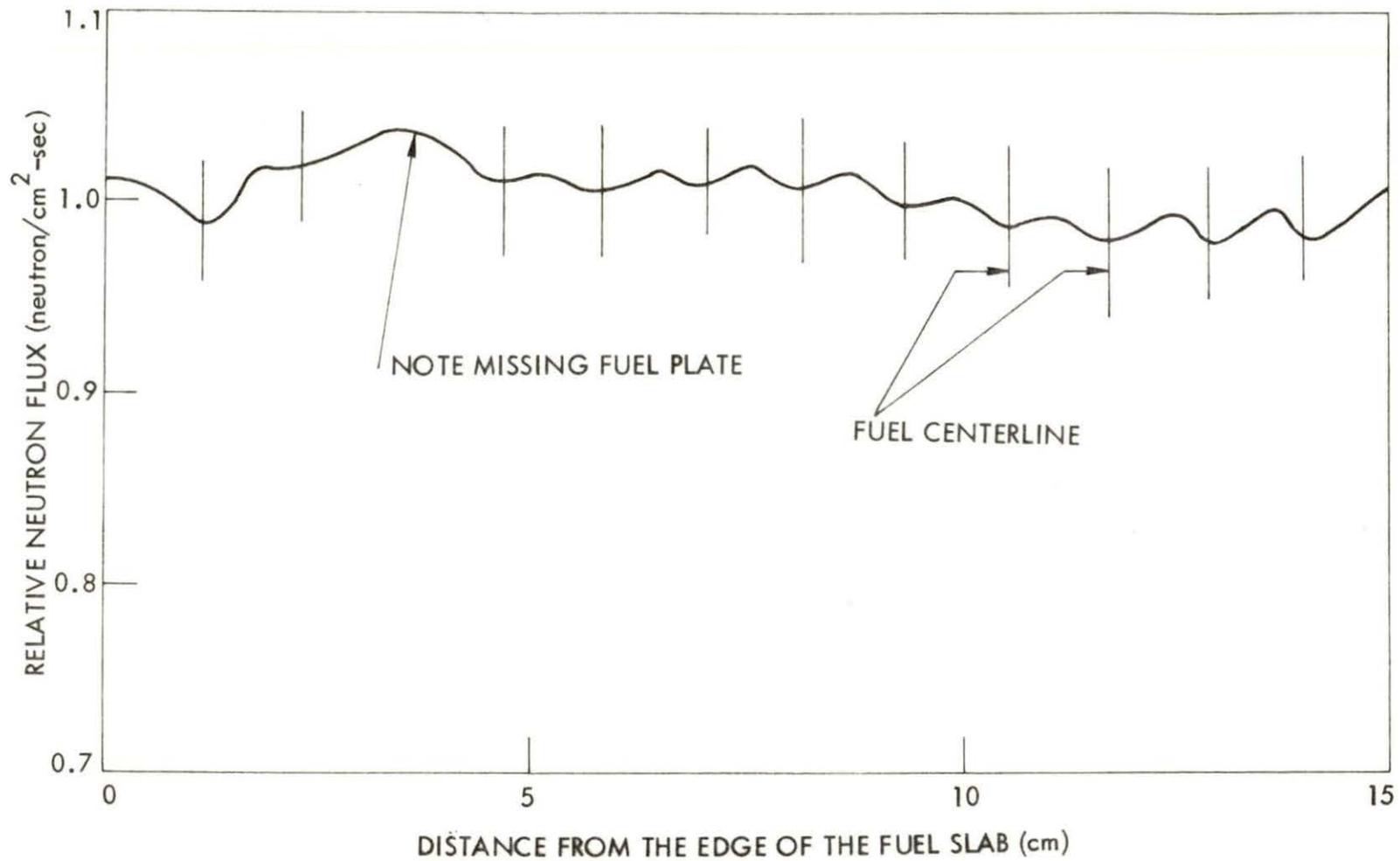
Fig. 5. Thermal neutron flux distribution in the fuel element of the South Core with one fuel plate withdrawn
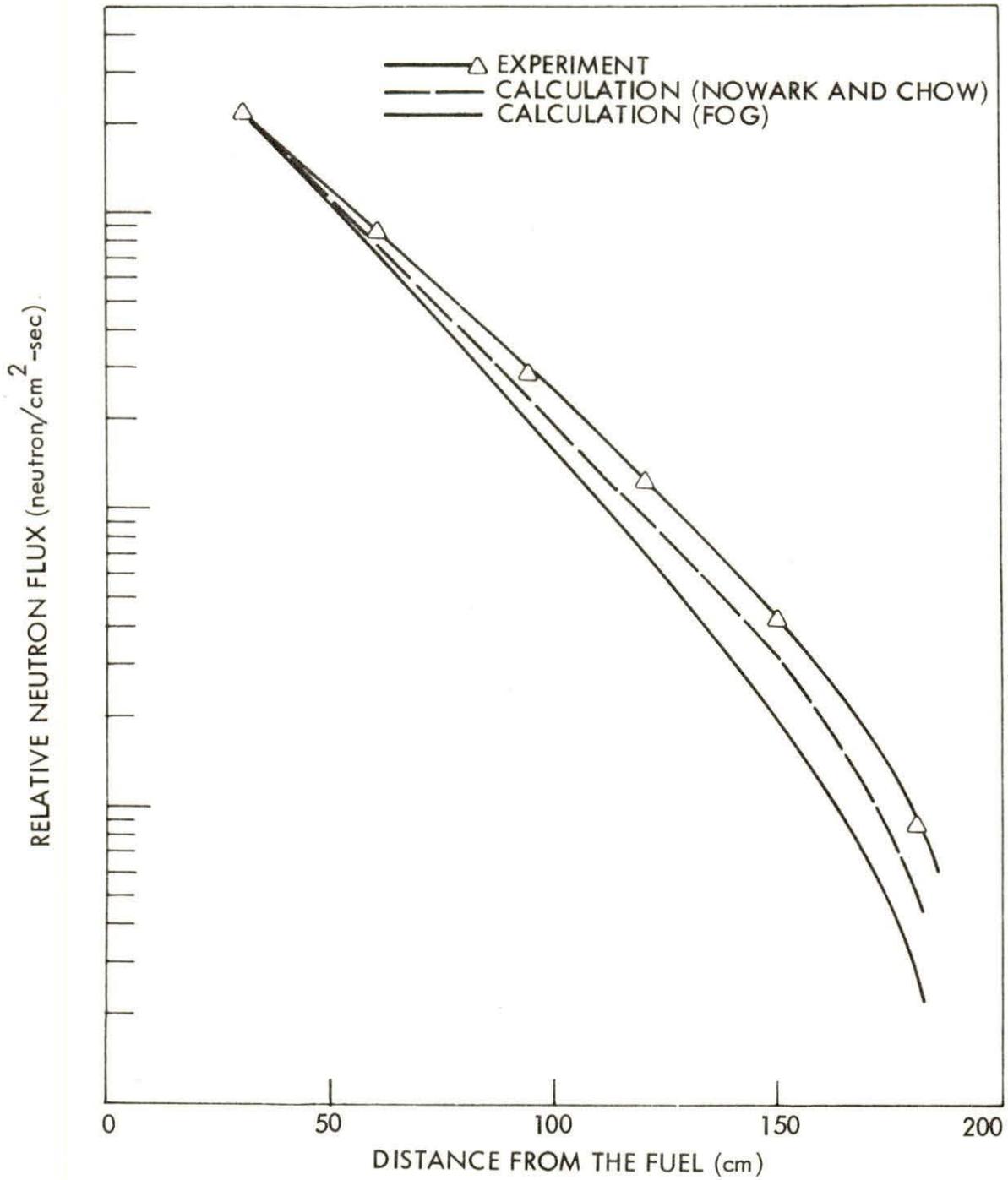
Fig. 6. Thermal neutron flux distribution in the thermal column of the UTR-10 reactor

probably due to the higher absorption corss section calculated by
LEOPARD. Depending on the concentration of impurities in commercial
graphite, cross sections have been reported over the range 0.00027 cm^{-1}
to 0.00040 cm^{-1}.

Due to the complicated geometry of the UTR-10, the exact value
of transverse buckling, necessary for the input of FOG, is hard to
determine.

By assuming the flux distribution in perpendicular directions
(horizontal and vertical) are cosine distribution, Moen [27] made a
horizontal and vertical flux profile through a core tank, extrapolating
the fluxes to zero and obtaining the transverse buckling as B^2 =
0.00325 cm^{-2}.

By the same assumption, Nowark and Chow [13] assumed the extra-
polated distance equal to reflector savings, the transverse buckling
found was B^2 = 0.00372 cm^{-2}.

A buckling search was performed by FOG to a desired eigenvalue
(1.005). The result found was B^2 = 0.00365 cm^{-2}.

Although the transverse buckling might be slightly smaller in
the graphite region than the fuel region, the transverse buckling
is assumed to be constant in this study.

C. Reactivity Coefficient Calculations

Inasmuch as safe operation of any nuclear reactor is closely
associated with the ability to predict the behavior of that reactor,
it will be shown that the calculations can predict core operational

conditions, and that the nuclear characteristics will have a high confidence level. The calculations were performed with the PERT code with LEOPARD and FOG input as described for reactivity calculation. Correlation of analysis with experiment will be presented to show that the reactor parameters are quite predictable.

1. Basis for confidence in LEOPARD

The calculational scheme described has been tested on a wide range of experimental lattices. Data from 56 metal and 55 oxide lattice critical and exponential experiments have been evaluated [4, 9]. The results of these studies are summarized in Table 11. The values of neutron multiplication k are computed using experimental measured material bucklings, and should equal unity. As the calculation accuracy is independent of variation in hydrogen to uranium ratio, uranium enrichment, pellet diameter and buckling, extrapolation from experiments to operating cores or extrapolation from one operating core to another should not lead to any significant error.

It can be seen from Table 11 that if only WAPD experimental results are considered, the computational method predicts k to a standard derivation of 0.36 percent.

2. Moderator void coefficient

A uniform void coefficient was calculated by assuming that a uniform change in the moderator atom density corresponds to a direct change in the amount of void present in the core. The expected range for this coefficient is reported in Table 12. The excess

Table 11. Results of calculations as a function of laboratory pro-
           viding experimental data

Laboratory	Type of experiment	No. of experiments	Calculated $k \pm \sigma$
Westinghouse Atomic Power Division (WAPD)	Critical	16	0.9968 ± 0.0036
Bettis Atomic Power Laboratory	Critical	14	0.9940 ± 0.0022
BNL	Exponential	35	0.9964 ± 0.0051
Handford	Exponential	20	0.9953 ± 0.0105
B & W	Critical	26	0.9885 ± 0.0094

Table 12. Reactivity changes in UTR-10

Description of change	Reactivity
1% of void in core tank	$- 8.36 \ (10^{-4})$
5% of void in core tank	$- 3.22 \ (10^{-3})$
10% of void in core tank	$- 6.34 \ (10^{-3})$
1% increase of fuel content	$4.20 \ (10^{-3})$
1 °F temperature rise	$- 5.90 \ (10^{-5})$

reactivity of the UTR-10 is 0.5%. It is shown that with 5% of void

in both core tanks, the reactor will be critical with all control

rods withdrawn.

3. Temperature coefficient

The temperature coefficient here is defined as the change in neutron multiplication per degree change in fuel and moderator temperature. The calculated value is $- 5.9 \times 10^{-5}$ $\Delta K/K/^oF$. The experimental results have been reported (R. A. Hendrickson, Nuclear Engr. Dept., ISU, private communication, 1974) are $- (5.0 \pm 1.0) \times 10^{-5}$ $\Delta K/K/^oF$. The two values are in good agreement.

4. Reactivity coefficient of additional fuel

The reactivity change due to 1% increase in fuel content is given in Table 12.

D. Prompt Neutron Lifetime and Effective Delayed Neutron Fraction

1. Prompt neutron lifetime

The calculated prompt neutron lifetime of the UTR-10 reactor is 130 μsec. Assume the magnitude of β is 0.0065, then the magnitude of α, which is defined as β/ℓ, is 50 rad/sec. Table 13 shows the theoretical calculation presented by Nowark and Chow [13], Nodean [16], Merritt [18] and the experimental results presented by Chan [17] and Nabavian [19].

The result calculated by PERT shows the good agreement with the experimental work.

2. Effective delayed neutron fraction

The effective delayed neutron fraction found was 0.0065. This seems to be in good agreement with nuclear data since the fuel is

highly enriched while the effect of delayed neutrons of U-238 is not pronounced.

Table 13. Comparison of calculated and experimental values of prompt neutron lifetime and alpha

	$\ell\,(\mu sec)$	$\alpha\,(rad/sec)$
PERT	130	50.0
Nowark and Chow	130	50.0
Nodean	130	50.0
Merritt	116-151	43.0-56.0
Chan	151	43.0
Nabavian	135-152	42.6-48.2

E. Comparison of the Cost

The cost of the SCORP code strongly depends on the type of problem. The SCORP code required 128K of memory and cost $2 to $3 per run (1974 cost) by object deck compared with $3 to $4.5 per run by FOG and PERT. Table 14 shows the cost of typical calculation of UTR-10.

Table 14. Comparison of the cost of computer codes

	Source deck	Object deck
FOG and PERT	$10.0	$3.6
SCORP	$ 6.0	$2.5

VI.   CONCLUSION AND SUGGESTION FOR FURTHER WORK

Within the scope of this study, it was found that reactor parameters such as temperature coefficient, prompt neutron lifetime and effective delayed neutron fraction are quite predictable. This shows that a computer code is a powerful tool for reactor analysis.

The main work of this study was developing the SCORP code, allowing single-step calculation of reactor parameters of interest rather than two-step calculation as usual. The essential advantage of the SCORP code is to simplify the FOG and PERT code, reduce the input data, thereby reducing the storage space required and the running time. The SCORP code can predict the flux distribution, reactivity change due to perturbation, prompt neutron lifetime and effective delayed neutron fraction with high level of confidence. The SCORP code will be a useful tool for the UTR-10 reactor parameter calculation.

However, there is always room for continual improvement, for example, modification of the subprogram in order to decrease the memory requirement, utilization of the updating numerical method, etc.

The subprogram of the code can be removed, modified and replaced without affecting the other sections. The following suggestions are made for the possible future work:

1.   Incorporate a subroutine to allow more than one perturbed region in perturbation calculation.

2.   Add option to calculate total heat generation in reactor.

VII. BIBLIOGRAPHY

1. R. F. Barry. 1963. LEOPARD — A Spectrum Depletion Non-Spatial Depletion Code for the IBM-7094. WAPD-3741, Westinghouse Electric Corporation, Atomic Power Div., Pittsburgh.

2. H. P. Flatt. 1961. The FOG One-Dimensional Neutron Diffusion Equation Codes. NAA-SR-6104, North American Aviation, Inc., Downey, Calif.

3. H. P. Flatt. 1960. PERT — A Perturbation Theory Code. NAA Program Description, North American Aviation, Inc., Downey, Calif.

4. Carolina Power and Light Company. H. B. Robinson Unit No. 2. 1966. Preliminary Facility Description and Safety Analysis Report. Carolina Power and Light Company, Lake Robinson, South Carolina.

5. A. Foderaro. 1959. Nucl. Sci. Eng. 6: 514.

6. H. Bohl, E. Gelard and G. Ryan. 1957. MUFT-4 — Fast Neutron Spectrum Code for the IBM-704. WAPD-TM-72, Westinghouse Electric Corporation, Atomic Power Div., Pittsburgh.

7. H. Amster and R. Suarez. 1957. The Calculation of Thermal Constants Averaged over a Wigner-Wilkins Flux Spectrum: Description of the SOFOCATE Code. WAPD-TM-39, Westinghouse Electric Corporation, Atomic Power Div., Pittsburgh.

8. W. H. Arnold. 1959. Critical Masses and Lattice Parameters of H_2O-UO_2 Critical Experiments: A Comparison of Theory and Experiment. YAEC-152, Yankee Atomic Electric Company, Boston.

9. L. E. Strawbridge. 1963. Calculation of Lattice Parameters and Criticality for Uniform Water Moderated Lattice. WCAP-3269-25, Westinghouse Electric Corporation, Atomic Power Div., Pittsburgh.

10. O. J. Marbowe and P. A. Omborellaro. 1957. CANDLE, A One-Dimensional Few Group Depletion Code for the IBM-704. WAPD-TM-53, Westinghouse Electric Corporation, Atomic Power Div., Pittsburgh.

11. H. P. Flatt and D. C. Baller. 1960. AIM-5, A Multigroup, One-Dimensional Diffusion Equation Code. NAA-SR-4694, North American Aviation, Inc., Downey, Calif.

12. S. T. Munson. 1973. The FOG Code. M.E. Paper, Dept. of Nuclear Engineering, Iowa State University.

13. M. J. Nowark and K. T. Chow. 1957. Reactor Physics of UTR-10. ASAE-19, American-Standard, Atomic Energy Div., Redwood City, Calif.

14. A. M. Campos. 1964. Thermal and Epithermal Flux Shapes in the Thermal Column of the UTR-10 Reactor. M.S. Thesis, Library, Iowa State University.

15. American Standard Company. 1959. Operating Manual of UTR-10 Reactor. American Standard Co., Redwood City, Calif.

16. W. C. Nodean. 1969. The Response of a Coupled Core Reactor to a Localized Oscillation of the Absorption Cross Section. Ph.D. Thesis, Library, Iowa State University.

17. T. C. Chan. 1971. Reactor Transfer Function Measurements with the Reactor Oscillator. M.S. Thesis, Library, Iowa State University.

18. I. W. Merritt. 1968. Spatially Dependent Frequency Response of Coupled-Core Reactors. Ph.D. Thesis, Library, Iowa State University.

19. M. Nabavian. 1973. Reactor Noise Measurements in the UTR-10 Using the Polarity Correlation Method. M.S. Thesis, Library, Iowa State University.

20. M. Clark and K. F. Hansen. 1964. Numerical Methods of Reactor Analysis. Academic Press Inc., New York.

21. H. P. Flatt. 1960. Finite Difference Approximations to the Neutron Diffusion Equation. NAA-SR-TOR-5889, North American Aviation, Inc., Downey, Calif.

22. D. Meneghetti. 1963. Introductory Fast Reactor Physics Analysis. ANL-6809, Argonne National Lab., Lemont, Ill.

23. H. Soodak. 1962. Reactor Handbook, Volume III, Part A. Interscience Publishers, New York.

24. D. Meneghetti. 1962. Recent Advances and Problems in Theoretical Analysis of ZPR-III Fast Critical Assemblies. Proc. Seminar on Physics of Fast and Intermediate Reactors, Paper SM-18/37. Vienna.

25. G. R. Keepin, T. F. Wimett, and R. K. Zeigler. 1957. Delayed Neutrons from Fissionable Isotopes of Uranium, Plutonium and Thorium. LA-2118, Los Alamos Scientific Lab., New Mexico.

26. G. R. Keepin, T. F. Wimett, and R. K. Zeigler. 1957. Delayed Neutrons from Fissionable Isotopes of Uranium, Plutonium and Thorium. Phys. Rev. 107: 1044.

27. D. A. Moen. 1971. Reactor Frequency Response Based on Pulsed Neutron Technique. Ph.D. Thesis, Library, Iowa State University.

VIII. ACKNOWLEDGMENTS

The author wishes to thank his major professor, Dr. Richard A. Hendrickson, for his support and interest throughout the course of this study.

The author also wishes to thank his parents, Mr. and Mrs. Lin-hai Chen, for their continued support and encouragement.

IX. APPENDIX A. INPUT DATA FOR SCORP

A. General Information of Input Data

The arrangement of the input cards must be as indicated below:

1. One title card.

2. One set of cards containing fixed-point data. Within this group of data, cards may be in any order; however, the final card must contain a "1" in column 1.

3. One set of cards containing floating-point data, cards may be in any order; however, the final card must contain a "1" in column 1.

4. One card containing alphanumeric information for perturbation problem identification.

5. One set of cards containing floating-point data, cards may be in any order; however, the final card must contain a "1" in column 1.

6. One or more cards containing floating-point data for material identification.

B. Detailed Description of Input Data

1. Title card

Any alphanumeric information not exceeding 72 characters may be used.

2.   Fixed-point data

Options for the real and adjoint flux calculation are included in this set of data. When the first entry to the program is made at the start of a problem, the fixed-point array and the floating-point data array are set equal to zero. Thus all options that are not set will be zero. For each card, the format is

Card format	Data description
I1	Left blank unless it is last card of fixed-point data, in which case the number "1" is placed in this column.
I11	Relative address of the first piece of data on card. All data following the first piece must be stored consecutively; however, if any data field is left blank, no change will be made in the memory location corresponding to this field.
5I12	Fixed-point data corresponding to relative address.

Relative address	Data description
	Number of groups
L(1)	Restriction: number of groups should not exceed 4.

Type of flux calculation

L(2)

0: Compute flux only

1: Compute flux and adjoint flux

2: Compute adjoint flux only

Boundary condition at origin

L(3)

0: $d\phi_i/dr = 0$

1: $\phi_i = 0$

2: $\phi_i = \omega_i'$

3: $\phi_i + \omega_i d\phi_i/dr = 0$, ω_i input data

4: $\phi_i + \omega_i d\phi_i/dr = 0$, ω_i computed by code

5: $\phi_i + \omega_i d\phi_i/dr = 0$, $\omega_i = -2.131338\ D_i$, computed by code

Boundary condition at outer boundary

L(4)

0: $\phi_i = 0$

1: $d\phi_i/dr = 0$

2: $\phi_i = \omega_i'$

3: $\phi_i + \omega_i' d\phi_i/dr = 0$, ω_i' computed by code

4: $\phi_i + \omega_i' d\phi_i/dr = 0$, ω_i' input data

5: $\phi_i + \omega_i' d\phi_i/dr = 0$, $\omega_i' = -2.131338\ D_i$, computed by code

Number of intervals

L(8)   The number of intervals in region 1

is stored here. The number of

intervals in the following regions

are stored consecutively.

Restriction: Total number of

intervals should not exceed 238.

Buckling by region

L(49)   0: Constant buckling, all regions

1: Region dependent

Criticality search

L(65)   0: No search

1: Buckling search

2: Poison search

Perturbation calculation

L(108)   0: No perturbation calculation

1: Calculate $\Delta K/K$ only

2: Calculate β_{eff}, ℓ only

3: Calculate $\Delta K/K$, β_{eff} and ℓ

3. Floating-point data

Reactor parameters for flux and adjoint flux calculation are in-
cluded in this set of data. The format for each card must be as
indicated below:

Card format	Data description
I1	Left blank unless it is last card of floating-point data, in which case the number "1" is placed in this column.
I11	Relative address of the first piece of data on card. All data following the first piece must be stored consecutively.
5F12	Floating-point data corresponding to relative address.

Relative address	Data description
A(1)	Convergence criterion ϵ_1 for flux calculations
A(2)	Convergence criterion ϵ_2 for criticality search
A(3)	The value of the eigenvalue to be searched for in criticality search. If this value is unity, it need not be entered.
A(4)	Convergence criterion for criticality search calculation.
A(7)	Initial value of coordinate system with respect to the origin. This value must be positive if extrapolated boundary is used.

A(8)	Values of width of each region.
A(50)	Values of buckling.
A(90)	Initial source guess in each region.
A(395)	For each group in order, values of χ_j.
A(600)	$(\Sigma_s)^1_{i,j \to j+1}$
A(800)	$(\nu\Sigma_f)^1_{i,j}$
A(1000)	$(\Sigma_a)^1_{i,j}$
A(1200)	$(D_{i,j})^1$

4. <u>Alphanumeric data</u>

This card is used for perturbation problem identification. Any alphanumeric information not exceeding 72 characters may be used.

5. <u>Floating-point data</u>

The card format is the same as part (3). The data required for calculation of $\Delta K/K$, β_{eff} and ℓ are entered here.

<u>Relative address</u>   <u>Data description</u>

B(1)   Region number in which the perturbation takes place

B(2)   Lower boundary of the part of the reactor which is being perturbed

---

[1]The subscripts i and j refer to region and group respectively. For example, there are 3 regions and 2 groups. $D_{i,j}$ must be read in the following order: $D_{1,1}$, $D_{2,1}$, $D_{3,1}$, D_{12}, D_{22}, D_{32}. Then the following relative address must be used:

$\qquad$ A(1200) — $D_{1,1}$
$\qquad$ A(1240) — $D_{1,2}$

B(3)	Upper boundary of the part of the reactor which is being perturbed
B(4)	Values of prompt neutron spectrum X_i
B(10)	For each group in order, values of $\delta(\frac{1}{D})$
B(15)	For each group in order, values of $\delta(\Sigma_a)$
B(20)	For each group in order, values of $\delta(\nu\Sigma_f)$
B(25)	For each group in order, values of $\delta(\Sigma_R)$
B(30)	Values of delayed neutron spectrum χ'
B(39)	Number of different materials. There may be at most five different materials.
B(40)	For each material in order, specify the number of fissionable isotopes. At most five different fissionable isotopes may be present in a given material.
B(45)	For each fissionable isotope, enter in order, β for that isotope.

B(50)

For each region in order, enter the material identification number in that region[1]

B(70)

The value for $\nu\Sigma_f$ for fissionable isotope number 1 is entered here beginning with group 1 in B(70). The values for the second fissionable isotope are entered in B(90), etc.

6. Material identification data

The identification numbers for each fissionable isotope and their corresponding atom fraction are entered in the manner indicated below. One data card is required for each material. The card format is 2I1, I10, 5(I2, F10.9). There are at most five different fissionable isotopes in a material.

Card format	Data description
I1	Number of fissionable isotopes for material #1
I1	Left blank unless it is the last card
I10	Relative address of first piece of data. For material #1, the address is 1; for material #2, the address is 11; for material #3, the address is 21, etc.

---

[1]If, for example, there are five regions in a reactor, region 2 and region 4 are fuel regions which contain material #1 and material #2 respectively, then the following data are used:

    0.0   1.0   0.0   2.0   0.0.

I2   Identification number of fissionable

isotope[1].

F10.9   Atom fraction of the fissionable

isotope.

---

[1]See Appendix C.

X. APPENDIX B. SCORP CODE OUTPUT

The printed output is divided into three parts, namely, input data edit, diffusion solution output, and perturbation solution output.

A. Input Data Edit

The first item of output is a direct listing of the input data including cross sections, dimensions, and the type of problem to be solved.

The program then reads and checks the data. Most parameters that would produce a meaningless result if incorrect are tested, and appropriate error messages are printed.

B. Diffusion Solution Results

Following the input data edit, the solution routines are entered; the eigenvalues from the last two inner iterations are printed. When the solution converges, the point-by-point sources and fluxes are listed. The above process is then repeated for the adjoint solution, if this option is used.

The program then checks the results. The following will be printed:

1. The volume of each region.

2. Integrated fluxes for each region and each group.

3. The integrated product of the flux and the adjoint flux for each region and each group if the adjoint flux is also computed.

4. The leakage and removal for each region and each group.

5. For each fuel region the peak-to-average flux and peak-to-average source for the thermal group only.

6. For entire reactor, the overall average flux and average source.

C. Perturbation Solution Results

Following the diffusion results, the program prints the data of the perturbation in cross sections and diffusion coefficients, along with the region and boundaries of the single region being perturbed.

Then the program prints the reactivity change along with the fraction of the reactivity change due to perturbation of fission, absorption, removal and diffusion parameters.

Finally, the delayed neutron fraction and prompt neutron life-time are printed.

XI. APPENDIX C. SAMPLE DATA FOR SCORP

In the sample data below, the reactor is not supposed to be realistic. The purpose is simply to illustrate the data format. Suppose the reactor had the following configuration:

Region 1: Reflector (graphite, 188 cm wide)

Region 2: Fuel (water moderator, 90% U-235, 8% U-238 and 2% Pu-239; 15 cm wide)

Region 3: Reflector (graphite, 45 cm wide)

Region 4: Fuel (water moderator, 92% U-235; 8% U-238; 15 cm wide)

Region 5: Reflector (graphite, 105 cm wide)

SAMPLE DATA FOR THE SCORP CODE

	1	2	1	4	4	1
	7	5				
	8	10	5	10	5	10
1	108	3				
	1	0.01	0.001	1.0	0.01	
	7	10.0				
	8	188.0	15.0	45.0	15.0	105.0
	50	0.0032				
	90	0.0	0.5	0.0	0.5	0.0
	395	1.0	0.0			
	600	0.003	0.037	0.003	0.038	0.003
	800	0.0	0.0021	0.0	0.0019	0.0
	840	0.0	0.088	0.0	0.092	0.0
	1000	0.0001	0.0021	0.0001	0.0023	0.001
	1040	0.0003	0.05	0.0003	0.05	0.0003
	1200	1.126	1.322	1.126	1.310	1.126
1	1240	0.995	0.193	0.995	0.186	0.995

REACTIVITY CHANGE DUE TO 1% OF VOID

	1	2.0	11.0	15.0	1.0	0.0
	10	-0.006	-0.05			
	15	0.0001	-0.0002			
	20	0.0	-0.001			
	25	-0.004	0.0			
	30	1.0	0.0			
	39	2.0	3.0	2.0		
	45	0.0065	0.0148	0.0021		
	50	0.0	1.0	0.0	2.0	0.0
	70	0.002	0.09			
	90	0.0001	0.0002			
1	110	0.0003	0.0004			
3	1	1 0.9	2 0.08	3 0.02		
21	11	1 0.92	2 0.08			